

Athermal Hybrid Silicon/Polymer Ring Resonator Electro-optic Modulator

Feng Qiu,[†] Andrew M. Spring,[†] Hiroki Miura,[‡] Daisuke Maeda,[§] Masa-aki Ozawa,[§] Keisuke Odoi,[§] and Shiyoshi Yokoyama^{*,†,‡}

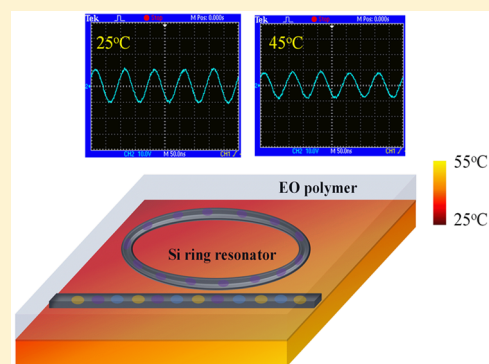
[†]Institute for Materials Chemistry and Engineering, Kyushu University, 6-1 Kasuga-koen Kasuga-city, Fukuoka 816-8580, Japan

[‡]Department of Molecular and Material Sciences, Kyushu University, 6-1 Kasuga-koen Kasuga-city, Fukuoka 816-8580, Japan

[§]Nissan Chemical Industries, LTD, 2-10-1 Tuboi Nishi, Funabashi, Chiba 274-8507, Japan

ABSTRACT: In this work, we have demonstrated a hybrid silicon/polymer ring resonator electro-optic (EO) modulator with a temperature-independent modulation. The waveguide consisted of an ultrathin silicon core with an EO polymer cladding. Using ultrathin silicon is advantageous, as it allows a reduction in the side-wall scattering loss and also offers excellent light distribution to enable athermal operation. With a radius of 60 μm , the ring exhibited a 9.7 dB extinction depth and a Q value of 1.25×10^4 . After poling of the EO polymer, the ring resonator functioned well as an EO modulator and operated in a stable manner between 25 and 55 $^{\circ}\text{C}$.

KEYWORDS: modulator, ring resonator, electro-optic polymer, silicon waveguide, athermal



The ring resonator is one of the most crucial optical components and is often used for the fabrication of compact photonic devices. Its applications include filters, switches, modulators, and other advanced on-chip optical elements.^{1–3} Silicon-based rings have attracted widespread attention due to their excellent compatibility with the world's most successful technology for producing electronics. Previous works have demonstrated the notable properties of silicon ring devices. They have highlighted advantages such as a low power consumption, wide bandwidth operation, and a compact footprint.^{4–6} Despite these numerous advantages, high-Q rings remain extremely sensitive to ambient temperature fluctuations as a consequence of the thermo-optic (TO) coefficient of silicon. With a positive TO coefficient of $1.8 \times 10^{-4}/^{\circ}\text{C}$, the resonance of the silicon ring consequently shows a strong temperature-dependent wavelength shift (TDWS) of 50–80 pm/ $^{\circ}\text{C}$.⁷ Thus, it is essential to diminish the TDWS difficulty by the utilization of an active thermal controller in the integrated device.⁸ This approach however may lead to a further power consumption problem. Recently, a dc bias-controlled silicon modulator has been demonstrated to work over a 7.5 $^{\circ}\text{C}$ temperature range with little additional power consumption.⁹ Another simple and effective way to overcome this issue is athermalization. This can reduce TDWS to almost zero by the use of suitable materials with a negative TO coefficient.^{8,10}

In this work, we have demonstrated a hybrid silicon and electro-optic (EO) polymer ring resonator modulator. Since the polymer has a negative TO coefficient, which is opposite the

silicon's positive coefficient, the resulting hybrid ring modulator has an athermal operation. A beam propagation calculation was carried out in order to design the optimal waveguide structure. The measured TDWS for the hybrid silicon and EO polymer ring resonator is only 2.1 pm/ $^{\circ}\text{C}$. With a V_{pp} of 4.0 V, the ring resonator has a 2–3 dB modulation depth over a temperature range between 25 and 55 $^{\circ}\text{C}$.

Figure 1a and b show the schematic of the designed ring resonator and the cross-section of the electrode-covered section, respectively. The waveguide consists of a silicon core with a height of 48 nm and a width of 2.0 μm . The thickness of the polymer cladding was 1.2 μm . Coplanar Au electrodes were utilized on top of the SiO_2 layer. The electrode separation is 6.0 μm , and the thickness 0.2 μm . For this waveguide the optical mode calculation was performed by using the quasi-TE mode. In the calculation, we entered the refractive indices of the EO polymer and silicon as 1.67 and 3.48, respectively. The cross-sectional distribution of the optical field intensity is shown in Figure 1c. The optical field is tightly concentrated around the silicon and partly penetrates into the EO polymer. Such a field distribution can be attributed to both the high refractive index contrast and the ultrathin silicon. The mode calculation indicates that the resulting optical field in the EO polymer overlaps with the horizontal dc field that was applied between the coplanar electrodes. Figure 1d shows the simulated electric field distribution between the coplanar electrodes, indicating

Received: December 4, 2015

Published: April 13, 2016

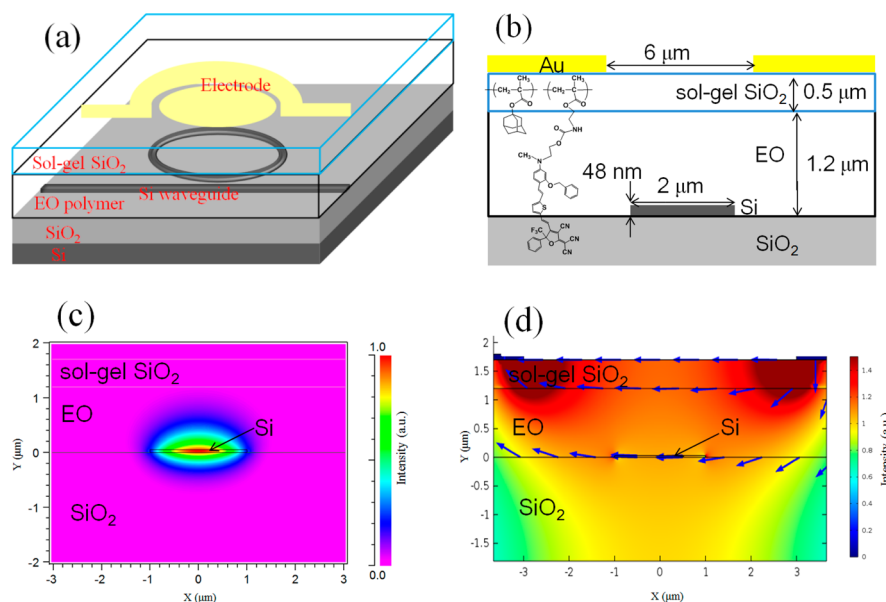


Figure 1. (a) Schematic of the designed ring resonator modulator, (b) cross-section of the electrode-covered section (inset shows the EO polymer structure), (c) simulated TE mode profile, and (d) distribution of the applied dc electric field (arrows denote the direction of the dc electric field).

that the continuous electric field reaches the silicon and EO polymer interface.

Generally, the athermal operation of a waveguide can be evaluated by using the following equation:

$$\frac{d\lambda_m}{dT} = \left(n_{\text{eff}} a_{\text{sub}} + \frac{dn_{\text{eff}}}{dT} \right) \lambda_m n_g \quad (1)$$

where $d\lambda_m/dT$ is the TDWS, λ_m the resonant wavelength, n_{eff} the effective refractive index of the waveguide, a_{sub} the substrate expansion coefficient, dn_{eff}/dT the TO coefficient, and n_g the group index of the waveguide.^{8,11} The refractive index and TO coefficient were 1.67 and $-1 \times 10^{-4}/^\circ\text{C}$ for the EO polymer, 3.48 and $1.8 \times 10^{-4}/^\circ\text{C}$ for the silicon, and 1.45 and $1 \times 10^{-5}/^\circ\text{C}$ for the SiO_2 . The a_{sub} of the SiO_2 substrate was $2.6 \times 10^{-6}/^\circ\text{C}$.⁷ In order to determine the optimal athermal condition in the hybrid waveguide, the change in TDWS as a function of the silicon thickness was plotted in Figure 2. It can be expected that the confinement factor denoted by the optical field intensity dispersed in the EO polymer will vary for each silicon thickness. Figure 2 indicates that the TDWS becomes zero when we

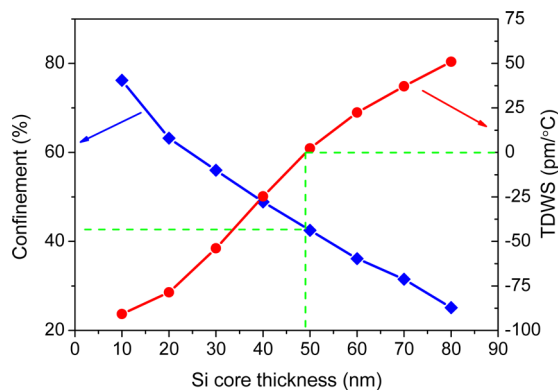


Figure 2. Calculated light confinement in the EO polymer layer and the TDWS of the waveguides with different silicon core thicknesses.

choose a $2 \mu\text{m}$ wide silicon core with a thickness of 48 nm, and in this structure the confinement factor is 42%.

To achieve a high-efficiency athermal silicon hybrid waveguide, it is essential for the light to be appropriately confined to the silicon core, cladding, and SiO_2 substrate. A silicon strip with dimensions of typically between 200 and 250 nm thickness and 250–500 nm width has been employed in previous athermalizations.^{7,8,12} We demonstrate here a hybrid ultrathin silicon and EO polymer ring resonator modulator, which promises superior advantages in terms of the propagation loss and EO activity. The propagation loss in silicon strip waveguides originates mainly from the sidewall roughness during the dry etching process. From the simulated TE mode distribution in Figure 1c, we can observe that the optical mode near the sidewall occupies only a small fraction of the total available optical field. On the other hand, a large optical field appears on the top surface of the silicon, which should be favorable to the EO operation.

The designed ring resonator was fabricated on an SOI substrate with a 200 nm thick silicon layer and a $5 \mu\text{m}$ thick SiO_2 layer. Initially, the silicon layer was thinned to the desired thickness by using inductively coupled plasma (ICP, SAMCO RIE-400iPB) etching with SF_6 gas. By considering the etching rate, we were able to control the etching time so that we could obtain a silicon layer with the desired thickness. The thickness of the silicon layer was found to be approximately 48 nm by using a stylus profiler (KLA-Tencor P15). Subsequently, the ring structure was patterned onto the silicon layer by using electron beam lithography (Elionix ELS7500) and ICP etching. The fabricated ring had a radius of $60 \mu\text{m}$ and a bus-ring gap of $0.3 \mu\text{m}$. After etching, the EO polymer (structure in Figure 1b) was spin-coated onto the substrate. After removal of the residual solvent by heating at 120°C for 24 h under vacuum, the film thickness was found to be $1.2 \mu\text{m}$. The EO polymer, which was prepared according to a modified procedure from our previous work,¹³ was known to exhibit a relatively high temperature resistance due to its elevated glass transition temperature of 168°C and its high thermal decomposition temperature of $\sim 210^\circ\text{C}$. A solution of sol-gel SiO_2 was spin-

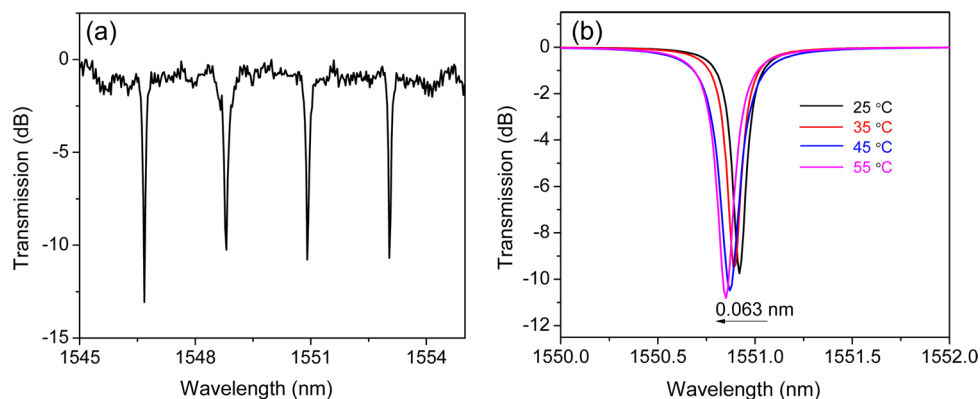


Figure 3. (a) Transmission spectrum of the ring resonator at 25 °C and (b) a collection of high-resolution spectra showing the change of one resonance peak over different temperatures.

coated onto the EO polymer layer and baked at 120 °C to form a 0.5 μm thick film.¹⁴ This thin sol–gel SiO_2 film acted as an effective buffer layer in order to minimize the absorption loss from the electrodes and to reduce any damage during the poling process. Finally, the coplanar electrodes that covered half of the ring, as can be observed schematically in Figure 1a, were deposited by sputtering from a Au target and using the lift-off technique.

To induce the EO effect, the EO polymer in the ring was poled at 160 °C by applying a dc voltage of 550 V to the electrodes. After poling, the transmission spectra of the ring resonator were measured by an end-fire coupling system. Light from a tunable laser source (Santec TLS-510) was coupled into the waveguide in TE mode through a polarization-maintaining lensed fiber, and the wavelength was scanned with a 10 pm step. To evaluate the athermal property, the device was placed on a heater and subjected to various temperatures of between 25 and 55 °C by using a thermoelectric temperature controller (ILX Lightwave LDT-5525). Finally the output light from the waveguide was collected using a second fiber and fed into a photodetector to obtain the transmission spectrum.

Figure 3a shows the transmission spectrum of the ring resonator measured at 25 °C. By analyzing the spectrum, the Q factor of the ring was found to be 1.25×10^4 with a resonance extinction depth of 9.5 dB for the resonance at around 1551 nm. The high Q depends on the ring structure and the optical loss; therefore we measured the propagation loss from the hybrid waveguide. By using a 20 mm long straight waveguide for the cut-back method, the propagation loss was found to be approximately 5.0 dB/cm. This propagation loss is relatively small when contrasted to the previous silicon-organic-hybrid waveguides with a slot or strip structure.^{15–17} The insertion loss of the device (fiber to fiber) was 25 dB, which can be improved by an enhanced mode matching between the fiber's spot and the waveguide dimension. Figure 3b displays the change in one resonant peak measured at different temperatures. The high-resolution spectra were obtained by fitting the measurements to a Lorentz function. We can observe that the spectral change is within a shift of 0.1 nm in the temperature range between 25 and 55 °C. By linear fitting of the resonant wavelength at various temperatures, the TDWS can be extracted as 2.1 pm/°C. As expected for the designed hybrid waveguide, the measured TDWS is 20–30 times lower than that of a pure silicon ring resonator waveguide.⁷

To perform the EO ring modulator, a dc electric field was applied to the electrodes and the resonance peak shift versus

the dc voltage was measured at 25 °C, as illustrated in Figure 4. The applied voltage ranged from –10 to 10 V with an interval

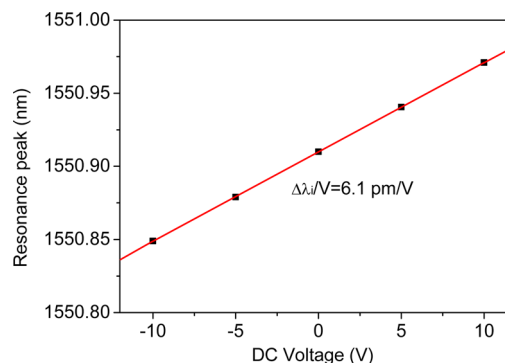


Figure 4. Resonance peak shift versus various dc voltages at room temperature.

of 5 V. After linear fitting the measured result, the resonance tunability $\Delta\lambda_i/V$ was found to be 6.1 pm/V, where $\Delta\lambda_i$ is the resonance peak shift and V is the applied dc voltage. In a ring resonator, the $\Delta\lambda_i$ is given by

$$\Delta\lambda_i = \frac{\lambda_i}{n_{\text{eff}}} \Delta n_{\text{neff}} \quad (2)$$

where λ_i is the one resonance peak wavelength and n_{eff} is the effective refractive index change.¹⁸ In the hybrid waveguide, $\Delta\lambda_i$ can be induced by the refractive index change of the EO polymer (Δn_{EO}), where the Δn_{EO} is expressed by

$$\Delta n_{\text{EO}} = \frac{1}{2} n_{\text{EO}}^3 r_{33} \frac{V}{d} \quad (3)$$

where V is the applied voltage and d is the interelectrode distance.¹⁸ By using eqs 2 and 3, the in-device EO coefficient (r_{33}) of the ring resonator modulator was calculated to be 48 pm/V.

In order to further evaluate the athermal operation of the fabricated ring resonator, high-frequency measurements were made by applying an ac field at various temperatures. The laser wavelength was scanned until the maximum in modulation depth was observed at 25 °C and then fixed at that point. With a 4 V_{pp} sine wave signal at 10 MHz, the light intensity modulation was induced with the extinction ratio of 3.3 dB, as shown in Figure 5. The extinction ratio of 3.1 dB was maintained at 35 °C, and 2.0 dB up to 55 °C. Since the TDWS

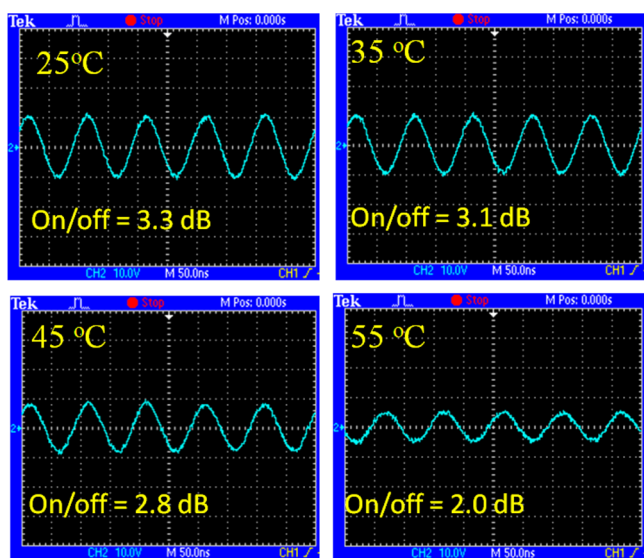


Figure 5. High-frequency response (10 MHz) at various temperatures.

of the fabricated ring resonator is a blue-shift, the athermal condition can be further improved through a more precise fabrication of the silicon waveguide to result in the ideal optical mode balance between these layers.

In conclusion, we have demonstrated the first example of a silicon ring modulator working over a 20–55 °C temperature range by the utilization of an EO polymer. We have presented in detail the design and procedure used to obtain an optimized ultrathin silicon/EO polymer ring resonator waveguide structure. The fabricated ring had a Q of 1.25×10^4 , an extinction depth of 9.7 dB, and a propagation loss of 5.0 dB/cm. The ring modulator exhibited a low TDWS of 2.1 pm/°C, and the EO polymer had an electro-optic frequency response of $r_{33} = 48$ pm/V. Our athermal waveguide structure may also be applicable to switching, filtering, and other on-chip resonator-based functionalities.

AUTHOR INFORMATION

Corresponding Author

*E-mail: s_yokoyama@cm.kyushu-u.ac.jp.

Notes

The authors declare no competing financial interest.

ACKNOWLEDGMENTS

This work was supported by the Cooperative Research Program of “Network Joint Research Center for Materials and Devices” of the Ministry of Education, Culture, Sports, and Science and Technology, Japan, and JSPS KAKENHI Grant Nos. 26289108 and 266220712.

REFERENCES

- (1) Reed, G. T.; Mashanovich, G.; Gardes, F. T.; Thomson, D. J. Silicon optical modulators. *Nat. Photonics* **2010**, *4*, 518–526.
- (2) Bogaerts, W.; De Heyn, P.; Van Vaerenbergh, T.; De Vos, K.; Kumar Selvaraja, S.; Claes, T.; Dumon, P.; Bienstman, P.; Van Thourhout, D.; Baets, R. Silicon microring resonators. *Laser Photonics Rev.* **2012**, *6*, 47–73.
- (3) Block, B. A.; Younkin, T. R.; Davids, P. S.; Reshotko, M. R.; Chang, P.; Polishak, B. M.; Huang, S.; Luo, J.; Jen, A. K. Y. Electro-optic polymer cladding ring resonator modulators. *Opt. Express* **2008**, *16*, 18326–18333.

- (4) Xu, Q.; Schmidt, B.; Pradhan, S.; Lipson, M. Micrometre-scale silicon electro-optic modulator. *Nature* **2005**, *435*, 325–327.

- (5) Baba, T.; Akiyama, S.; Imai, M.; Hirayama, N.; Takahashi, H.; Noguchi, Y.; Horikawa, T.; Usuki, T. 50-Gb/s ring-resonator-based silicon modulator. *Opt. Express* **2013**, *21*, 11869–11876.

- (6) Marris-Morini, D.; Baudot, C.; Fédéli, J.-M.; Rasigade, G.; Vulliet, N.; Souhaité, A.; Ziebell, M.; Rivallin, P.; Olivier, S.; Crozat, P.; Le Roux, X.; Bouville, D.; Menezo, S.; Boeuf, F.; Vivien, L. Low loss 40 Gbit/s silicon modulator based on interleaved junctions and fabricated on 300 mm SOI wafers. *Opt. Express* **2013**, *21* (19), 22471–22475.

- (7) Teng, J.; Dumon, P.; Bogaerts, W.; Zhang, H.; Jian, X.; Han, X.; Zhao, M.; Morthier, G.; Baets, R. Athermal silicon-on-insulator ring resonators by overlaying a polymer cladding on narrowed waveguides. *Opt. Express* **2009**, *17*, 14627–14633.

- (8) Padmaraju, K.; Bergman, K. Resolving the thermal challenges for silicon microring resonator devices. *Nanophotonics* **2013**, *2*, 1–14.

- (9) Timurdogan, E.; Sorace-Agaskar, C. M.; Sun, J.; Hosseini, E. S.; Biberman, A.; Watts, M. R. An ultralow power athermal silicon modulator. *Nat. Commun.* **2014**, *5*, 1–11.

- (10) Qiu, F.; Spring, A. M.; Yokoyama, S. An athermal and high- Q hybrid TiO_2 - Si_3N_4 ring resonator via an etching-free fabrication technique. *ACS Photonics* **2015**, *2*, 405–409.

- (11) Kokubun, Y.; Yoneda, S.; Tanaka, H. Temperature-independent narrowband optical filter at 1.31 μm wavelength by an athermal waveguide. *Electron. Lett.* **1996**, *32*, 1998–2000.

- (12) Djordjevic, S. S.; Shang, K.; Guan, B.; Cheung, S. T. S.; Liao, L.; Basak, J.; Liu, H.-F.; Yoo, S. J. B. CMOS-compatible, athermal silicon ring modulators clad with titanium dioxide. *Opt. Express* **2013**, *21*, 13958–13968.

- (13) Piao, X.; Zhang, Z.; Mori, Y.; Koishi, M.; Nakaya, A.; Inoue, S.; Aoki, I.; Otomo, A.; Yokoyama, S. Nonlinear optical side-chain polymers postfunctionalized with high- β chromophores exhibiting large electro-optic property. *J. Polym. Sci., Part A: Polym. Chem.* **2011**, *49*, 47.

- (14) Qiu, F.; Spring, A. M.; Yu, F.; Aoki, I.; Otomo, A.; Yokoyama, S. TiO_2 ring-resonator-based EO polymer modulator. *Opt. Express* **2014**, *22*, 14101–14107.

- (15) Himmelhuber, R.; Herrera, O. D.; Voorakaranam, R.; Li, L.; Jones, A. M.; Norwood, R. A.; Luo, J.; Jen, A. K.-Y.; Peyghambarian, N. A silicon-polymer hybrid modulator—design, simulation and proof of principle. *J. Lightwave Technol.* **2013**, *24*, 4067–4072.

- (16) Alloatti, L.; Korn, D.; Palmer, R.; Hillerkuss, D.; Li, J.; Barklund, A.; Dinu, R.; Wieland, J.; Fournier, M.; Fedeli, J.; Yu, H.; Bogaerts, W.; Dumon, P.; Baets, R.; Koos, C.; Freude, W.; Leuthold, J. 42.7 Gbit/s electro-optic modulator in silicon technology. *Opt. Express* **2011**, *19*, 11841–11851.

- (17) Gould, M.; Baehr-Jones, T.; Ding, R.; Huang, S.; Luo, J.; Jen, A. K.-Y.; Fedeli, J.-M.; Fournier, M.; Hochberg, M. Silicon-polymer hybrid slot waveguide ring-resonator modulator. *Opt. Express* **2011**, *19*, 3952–3961.

- (18) Qiu, F.; Spring, A. M.; Yu, F.; Aoki, I.; Otomo, A.; Yokoyama, S. Electro-optic polymer/titanium dioxide hybrid core ring resonator modulators. *Laser Photonics Rev.* **2013**, *7*, 84–88.